

Dynamically Produced Moving Groups in Interacting Simulations

PETER CRAIG,¹ SUKANYA CHAKRABARTI,¹ HEIDI JO NEWBERG,² AND ALICE QUILLEN³

¹*Rochester Institute of Technology*

²*Rensselaer Polytechnic Institute*

³*University of Rochester*

ABSTRACT

We show that Smoothed Particle Hydrodynamics (SPH) simulations of dwarf galaxies interacting with a Milky Way-like disk produce moving groups in the simulated stellar disk. We compare the observed disk moving groups in the Solar neighborhood with velocity perturbations produced in SPH simulations with and without dwarf galaxy interactions. Our simulations include three different cases: one that includes three satellites – with a Sagittarius-like dwarf galaxy interaction, as well as the Large and Small Magellanic Clouds; another that orbits in the plane of the Milky Way, and a null case, i.e., one with no dwarf galaxy interaction. The velocity sub-structures are identified using an algorithm to identify moving groups based on velocity over-densities in the plane of the disk. The properties of the identified moving groups change as the interacting simulations evolve. There are clear differences in the number and distribution of moving groups formed in the interacting simulations relative to the isolated simulation that we have analyzed. Our analysis suggests that some of the moving groups in the Milky Way may have formed due to dynamical interactions with perturbing dwarf satellites.

Keywords: XXXX XXXXX XXXX

1. INTRODUCTION

Moving groups have been observed in the local region of the Milky Way for many years. Many of these groups are quite well known, including the Hyades, Pleiades, Coma Bernices and Sirius moving groups (Eggen 1965). Parallaxes and proper motions from the Hipparcos satellite (ESA 1997) were particularly useful for identifying disk moving groups (Dehnen 1998). Gaia has significantly increased our ability to search for moving groups near the sun (Gaia Collaboration et al. 2018). Recent surveys have also added the line-of-sight velocity to the proper motions to provide full 3D velocity information for stars in the Solar neighborhood (Gontcharov 2006), which is needed to search for moving groups.

Several mechanisms for the formation of moving groups have been suggested. A common explanation is that moving groups are the remnants of open clusters, or formed by interactions with a bar (Dehnen 2000a). One problem with the cluster formation idea is that stars in moving groups can have a variety of different ages and compositions, so it is unlikely that they all came from the same cluster. An alternate scenario is that moving groups were formed through some kind of dynamical process, such as an interaction with the Galactic bar or a perturbing dwarf galaxy. It has been suggested that these groups are a result of perturbations from the Magellanic Clouds via gravitational interactions (Dehnen 1998). Analysis of GALAH data (Quillen et al. 2018b) suggests that some moving groups, such as the Hercules moving group, may be due to a resonant bar. Recent work also finds that transient spiral structure (Hunt et al. 2018) may lead to the formation of moving groups. It is likely that there may be multiple causal mechanisms at play in the formation of moving groups in the Milky Way.

Here, we explore the formation of moving groups in SPH simulations of the Milky Way interacting with satellites, and contrast this case with isolated simulations to understand the differences in their evolution and structural appearance. Earlier work (Quillen et al. 2009) used test particle calculations to study the formation of moving groups in an interacting simulation with a perturbing satellite. Hybrid techniques (incorporating both massive and tracer particles) used to simulate the Galactic disk also produce moving groups that resemble the Hercules stream (Quillen

Object	x (kpc)	y (kpc)	z (kpc)	vx (km/s)	vy (km/s)	vz (km/s)
Sagittarius	29.6	0.58	-15.8	-66.6	30.1	164.6
LMC	48.8	259.2	-67.0	-31.7	-235.4	-2.80
SMC	-10.7	184.2	4.6	40.3	-136.4	81.7
Coplanar	97.5	21.2	1.2	-251.8	-23.8	0.2

Table 1. Initial positions and velocities for the satellites in our simulations.

et al. 2011). Our focus on analyzing moving groups in the U-V plane is complementary to other recent work, including Khanna et al. (2019a) and Laporte et al. (2019) who have recently carried out analysis of Gaia DR-2 data, with a focus on understanding the structures in the $\langle Z - V_z \rangle$ plane.

The co-planar dwarf galaxy interaction that we examine here is adopted from our prior work (Chakrabarti & Blitz 2009), which led to the prediction of a new dark-matter dominated dwarf galaxy on an orbit with a close pericenter (< 10 kpc) to explain the observed large planar disturbances in the outer HI disk of the Milky Way (Levine et al. 2006). This interaction is similar to the one in Chakrabarti et al. (2019) for the recently discovered Antila2 dwarf galaxy, and Antila2’s current radial location matches our earlier prediction (Chakrabarti & Blitz 2009). If Antila2 is indeed the dwarf galaxy predicted earlier, as we discuss later some of the dynamically created velocity sub-structures in the solar neighborhood may be the result of this interaction. The simulations we analyze here are similar to ones that successfully reproduce the location and mass of a dwarf galaxy based on analysis of disturbances in the outer HI disks of galaxies (Chakrabarti et al. 2011). We also analyze a simulation that includes the three main tidal players of the Milky Way – the Large Magellanic Cloud (LMC), the Small Magellanic Cloud (SMC), as well as the Sagittarius (Sgr) dwarf galaxy. In all the interacting simulations, moving group structures form in the disk of the galaxy shortly after the dwarf galaxy begins to perturb the disk, and as we discuss below, their distribution and number differ from those in isolated simulations.

This paper is organized as follows. In §2, we review the simulation methodology, and in §3 we review the algorithm that we use here to characterize moving groups. In §4, we discuss the general characteristics of the moving groups found in our simulations, contrasting the interacting and isolated simulations. In §5, we apply our moving group algorithm to Hipparcos data and show that it does recover several well known moving groups. In §6, we qualitatively compare moving groups formed in these simulations to those found in the Milky Way. We discuss and present our conclusions in §7.

2. SIMULATIONS

We analyze three different kinds of simulations here. One simulation includes the LMC and SMC, as well as the Sagittarius dwarf galaxy. The progenitor mass of the Sagittarius dwarf in this simulation is $2.89 \times 10^{10} M_\odot$, and the progenitor masses for the LMC and SMC are $1.90 \times 10^{10} M_\odot$ and $0.19 \times 10^{10} M_\odot$ respectively. The initial conditions and orbits for these three dwarf galaxies have been derived using HST proper motions (Lipnicky & Chakrabarti 2017). Starting with the observed positions and velocities at present day, we carry out a backward integration in a galactic potential (the Hernquist profile matched to NFW as described in Springel et al. (2005)) using an orbit integration code (Chang & Chakrabarti 2011). Over relatively short timescales (\sim Gyr), evolving the simulation forwards with these initial conditions in a live halo will produce approximately accurate locations for the dwarf galaxies at present day (Chakrabarti et al. 2019). The Sgr dwarf experiences two pericenters over the last three Gyr, with the most pericenter occurring 0.3 Gyr before present day; the LMC and SMC have not approached closer than ~ 50 kpc relative to the Galactic disk over the last few Gyr, as found also in earlier work (Besla et al. 2012)).

The co-planar simulation that we analyze here includes a massive dwarf ($M_{\text{dwarf}} \sim 10^{10} M_\odot$) progenitor with an orbital plane that is nearly in the disk (Chakrabarti & Blitz 2009), and a close pericenter approach (~ 8 kpc). This close pericenter approach occurs 0.3 Gyr before present day. The third simulation does not have a perturber, and we use this “null” simulation as a point of contrast to the interacting galaxy simulations. We analyze the simulation output files at intervals of 50 Myr. Table 1 shows the starting positions and velocities for all of the satellites in these simulations.

As in prior work (Chakrabarti & Blitz 2009), we use a Hernquist profile matched to the NFW profile (Springel et al. 2005) to simulate the dark matter halo of the Milky-Way like galaxy. We use a concentration of 9.4, a spin parameter of $\lambda = 0.036$ and a circular velocity $V_{200} = 160 \text{ km s}^{-1}$. We also include an exponential disk of gas and stars, as well as an extended HI disk. The disk mass fraction is 4.6% of the total mass, which results in a radial scale length for the exponential disk of 4.1 kpc. The mass fraction of the extended HI disk relative to the total gas mass is 0.3, with a scale length that is three times that of the exponential disk Chakrabarti & Blitz (2009).

We have utilized the parallel TreeSPH code GADGET-2 (Springel 2005) to create simulations of a Milky Way-like galaxy interacting with satellites. GADGET uses an N-body method to simulate the collisionless components (the dark matter and stars) and Smoothed Particle Hydrodynamics (SPH) to follow the evolution of the gaseous component. The gravitational softening lengths are 100 pc for the gas and stars and 200 pc for the dark matter halo particles. In the primary galaxy, we use 4×10^5 gas and stellar particles and 1.2×10^6 dark matter halo particles. The model is initialized with a stellar mass of $3.5 \times 10^{10} M_\odot$, a gas mass of $1.25 \times 10^{10} M_\odot$, and a dark matter mass of $1.44 \times 10^{12} M_\odot$. These galactic components are represented in the simulation by different particle types, which are gas, disk, halo and new star particles. Disk particles represent the stellar component of the galaxy which is present at the start of the simulation; these stars do not evolve over time. As the simulation progresses, the simulation gas can be converted into new stars following a Kennicutt-Schmidt prescription for star formation.

Our version of GADGET-2 uses an effective equation of state (Springel & Hernquist 2003) where a subresolution model is adopted for energy injection from supernovae. Star formation is modeled using the Kennicutt-Schmidt algorithm. We adopt a value of 0.75 for the bulk artificial viscosity parameter and the details of the implementation of the viscosity is described in Springel (2005).

Face-on renderings of the simulated Milky Way at present day for the gas and stellar density distribution are shown in Figure 1 for the co-planar simulation and in Figure 2 for the simulation with the LMC, SMC, and the Sgr dwarf. The Fourier amplitudes for the spiral structure in this simulation can be found in Chakrabarti & Blitz (2009). Typical values for the Fourier amplitudes of the gas surface density range of the low-order modes in the outer HI disk are ~ 0.2 , with comparable values for the stellar disk. It is likely that over the time-scales explored in this paper, where moving group formation correlates closely with the interaction with the satellite, the role of gas dynamics (i.e., dissipation and angular momentum transport to the stars) is not significant.

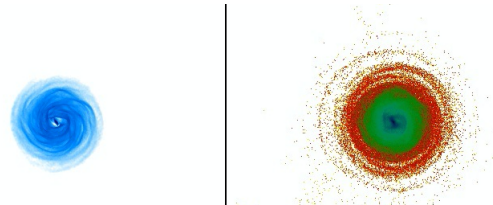


Figure 1. (Left) Gas density map at present day in the co-planar simulation. (Right) Stellar density map at present day in the co-planar simulation

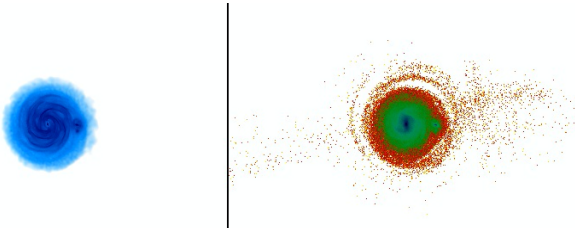


Figure 2. (Left) Gas density map at present day in the simulation with the three satellites (LMC, SMC, and a Sgr interaction). (Right) Stellar density map at present day.

3. ALGORITHM

We developed a method to find and characterize groups in various data sets in an automated fashion given the large quantity of data. Initially, we attempted to use a convergent point algorithm to identify moving groups, which posits that stars with comparable 3D space velocities will have proper motions that cause them all to converge to a single point on the sky. However, this algorithm did not work well for our purposes, because it is biased towards stars with low proper motions. For observed data, this method has the nice benefit of only requiring proper motions, and not radial velocities, but for our purposes it is better to have a method that eliminates the bias towards more distant objects, and since we have exact 3D velocities for all the particles in the simulation, this benefit is less useful.

Several other methods have been used for the analysis of velocity structures, most notably a wavelet analysis, as in [Ramos et al. \(2018\)](#). These methods are quite effective in large data sets like the GAIA RVs sample ([Gaia Collaboration et al. 2016, 2018; Soubiran et al. 2018; Katz et al. 2019](#)). A method like this is relatively appealing for our purposes, and our algorithm to identify moving groups, given data with full 3D velocity information (although we quickly reduce this to the components of the velocity in the U and V directions), is similar to this method. For each identified group, the average velocity, velocity dispersion, and stellar fraction is determined. We have applied the same algorithm on data for observed stars in the Solar neighborhood, and for stars selected from regions of each simulation that are similar to the Solar neighborhood in distance from the Galactic center.

We fit a series of Gaussian distributions to the (U, V) velocities, where U points towards the center of the Milky Way and V points in the direction of motion of a typical star on a circular orbit. The algorithm begins by binning the 2 dimensional data into a 2D histogram. Then we fit one large, axis-aligned Gaussian, with a center and width determined by the average and standard deviation of the data set in each direction. We then can search for regions in the $U - V$ plane that have an appreciably higher density than this one Gaussian profile. This is done simply by evaluating the Gaussian profile in each bin, and then subtracting that amount from the observed star count. Bins with large residuals are most likely part of a moving group.

We then fit additional Gaussian distributions, usually containing fewer stars than the original Gaussian, and with smaller standard deviations. Each of these Gaussian distributions describes one of the groups within the data set. Each of the Gaussian distributions added here has a total of five parameters: a center location in the U and V directions, standard deviations in these directions, and one parameter for the amplitude of the Gaussian. The parameters for these distributions are found by removing the background stars and then looking for over-densities in the remaining distribution. The center parameters are simply set by finding the center of an over-density. This allows us to fit a distribution on top of each group in the data set. This usually produces some false-positives due to over-densities caused by random noise.

The parameters for these groups are then fine-tuned using an optimization algorithm from `scipy.optimize.minimize`. The algorithm uses a two sided Kolmogorov-Smirnov test implemented in Scipy in order to evaluate the fit of the distribution to the data. Most of the parameters are reasonably close to the correct values already, however the standard deviations are sometimes inaccurate, which is remedied by the optimization routine. We can also determine the fraction by subtracting out our final distribution for this group until there is no longer an over-density at that location. These optimizations are done for the groups one at a time, where the parameters for all of the other distributions are held constant. Ideally we would be able to fit them all at once, but this is very computationally expensive. The exception is that if two groups are close enough to effect each other, then we optimize them together. This is usually not the case for any of the groups, but this condition is triggered if the two groups have estimated centers that are within 10 kilometers per second.

At this point the algorithm will have identified the locations of every group in the data set, but it also will have many false positives, which need to be removed. We do this is by comparing the number of stars in the central region of the group to the number we expect in that region from the background. If there are considerably more stars present than what we expect based on the background, we determine that it is a group. The threshold here is determined by subtracting out the background from all of our velocity bins, and then determining the standard deviation of the residual values. A value more than twice this standard deviation is sufficient to classify an over-density as a group. This was selected as it is strong enough to eliminate many of the false positives, while still identifying known structures

in the Hipparcos data set. This eliminates all of the cases where the algorithm has identified a velocity structure that is most likely random noise. This algorithm also requires that any group have at least 3 particles, which prevents any one particle with a high velocity from being classified as a group. A potential difficulty faced by this algorithm is that there is a dependence on the number of stars, which can make the comparison of the Milky Way and the simulations difficult, as the number of particles in the simulations within the solar neighborhood is less than the number of stars in the solar neighborhood with data in Gaia DR-2. However, as we discuss below, we find in practice that this is only a problem for very small moving groups.

4. GROUPS IN THE SIMULATIONS

Figure 3 shows the U and V velocities for the disk stars in our co-planar simulation, where U points towards the Galactic center, V points in the direction of the Sun’s motion around the Galactic center, and W is out of the plane of the Milky Way. The velocity dispersion in the z direction is much lower than in the others, which makes the velocity substructures relatively uninteresting. The stars included in this figure are only the stars that have existed since the beginning of the simulation, i.e., none of the newly generated stars are included. The data here is selected from a spherical region with a radius of 1 kpc centered at a location about where the Sun would be in the Milky Way. Figures 4 and 5 show similar plots for the remaining two simulations, with figure 4 showing the U and V velocities for the Sagittarius simulation. Similar plots can be generated including information about behavior in the W direction, however there is limited interesting behavior in that direction. We note that we recover similar structures, (but not as detailed due to our lower resolution) in the $\langle Z - V_z \rangle$ plane as [Laporte et al. \(2018\)](#) and [Khanna et al. \(2019b\)](#). The presence of the "vertical waves" in the stellar disk discussed in these and earlier papers ([Xu et al. 2015](#)) manifests itself in the $\langle Z - V_z \rangle$ representation, but not in the U-W or V-W representations.

In the Milky Way, data selection for moving groups typically involves a color cut in B-V. There are some differences noted in different cuts, and we look for similar behavior in the simulations. Although we have not post-processed our simulations to calculate the colors of the star particles, we can approximate a similar selection criteria by selecting particular age groups. We do not see significant differences in moving group formation when we include the new stars in addition to the old stars in our simulations. Carrying out this analysis using only the newly formed stars in the simulations gives similar results as those shown here. However, using only newly formed stars to find moving groups is occasionally problematic, especially early in the simulations when there are not as many new star particles. There are other times where the background distribution for the new stars is not well behaved, when identifying groups becomes more difficult. In our analysis here, we employ the old stars to identify moving groups in our simulations.

The fiducial region of the simulations that we sample in all our analyses is located at $x = 8$ kpc and $y = 0$ kpc, and we select stars by choosing all stars within a sphere with a radius of 1 kpc from this location. This selection is meant to simulate the region around the Sun in which we observe moving groups. This is one of several regions sampled in each simulation, with similar behavior exhibited in axially symmetric places around the disk. All of the sampled regions are at a radius of 8 kpc from the Galactic center, and each of the sampled regions shows similar general trends. There is usually only limited group formation within the first 500 Myr of the simulation, before the perturber has made a close pass. In these simulations, the groups disappear within a single (50 Myr) time step, and we cannot track one of these groups over time. With higher time resolution it should be possible to identify the time dependence of the moving groups.

It is worth noting that the number of groups found in the simulations is roughly a third (for the co-planar case) to about half (for the Sgr dwarf case) as many as the number of groups in the Milky Way. This may be due to the fact that these simulations only include one dwarf galaxy interaction and not all of the satellites around the Milky Way. It is also likely due to the relatively low resolution of these simulations relative to the number of stars present in current data for the moving groups seen in the Milky Way. Moreover, other causal mechanisms for the formation of moving groups are not manifest in these simulations, i.e., moving groups can also form as a result of a dissipating open cluster or dynamical interactions with a bar ([Quillen et al. 2018a](#); [Dehnen 2000b](#)). In fact, the total velocity structure is likely built from a combination of secular dynamical effects, as well as from the perturbations of dwarf galaxies. Groups can form without interactions from an external perturbation, but are not manifest in our simu-

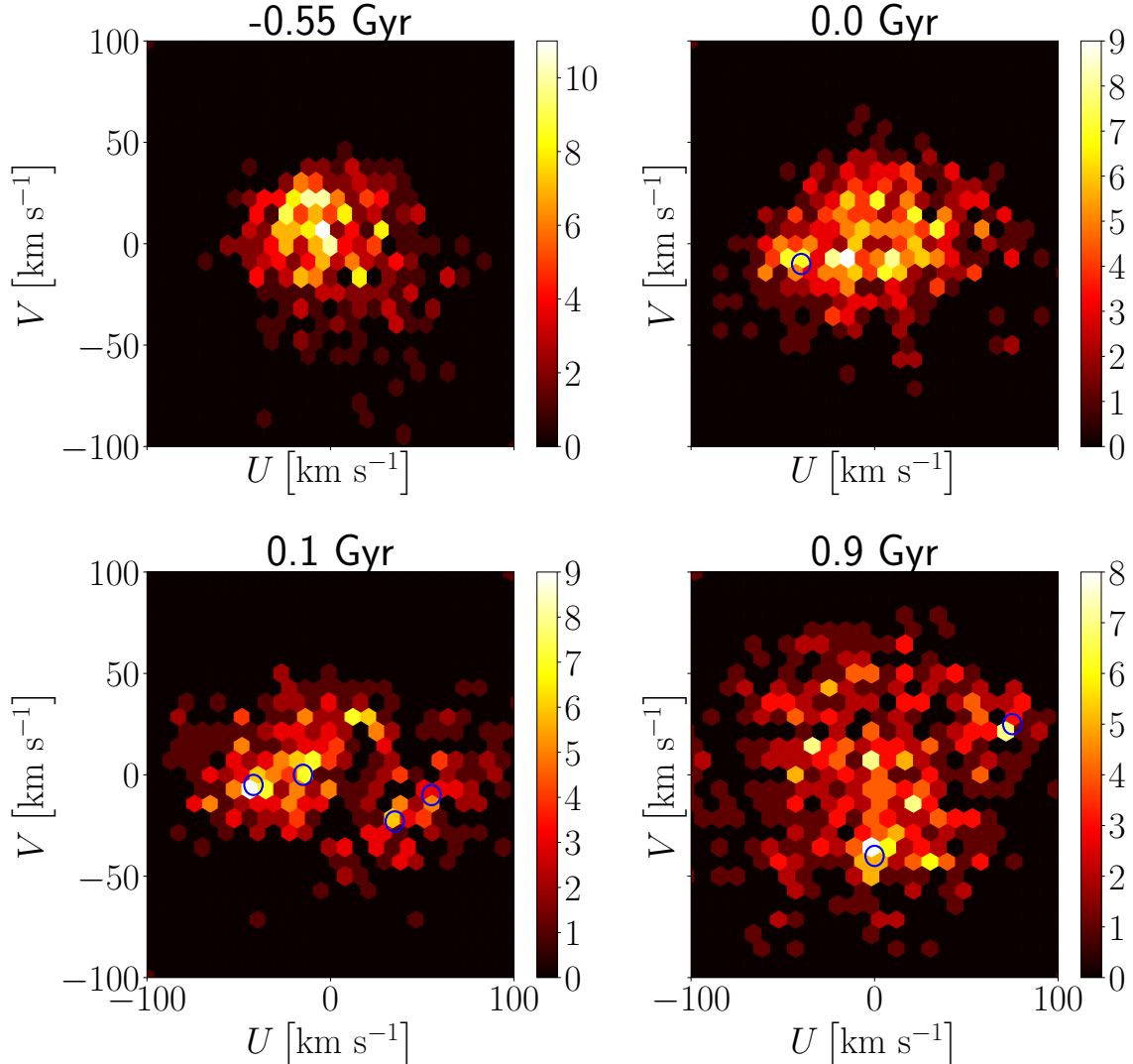


Figure 3. U and V velocities for stars in the disk for the simulation with a co-planar dwarf galaxy. The time labels are with respect to present day in the simulation. Here we see the clear formation of velocity substructure beginning near present day, which is shortly after the collision with the dwarf galaxy. The data shown is drawn from a spherical region of the disk 1 kpc in radius 8 kpc from the center of the galaxy. Similar results are obtained by using regions at different position angles inside of the disk. The time from present day is noted in each figure, with negative values occurring earlier in the simulations.

lations, so we should expect to have a lower number of moving groups form in these simulations relative to observations.

Interesting behavior can be seen from examining the number of groups as a function of radius. Our expectation is that the null simulations would have both a smaller number of velocity sub-structures and fewer sub-structures at larger radial locations. Figure 6 depicts the average number of groups in each simulation at the present day. We calculate this average by selecting eight different angles in the disk, then measuring the number of groups at a given radius across all eight angles and averaging those values. Each individual measurement is made using all of the disk stars located within a sphere with a radius of 1 kpc. As is clear, the interacting simulations have a larger number of moving groups relative to the null simulation, *and* a larger number of moving groups at all radii out to 10 kpc from the galactic center. Given the particularly low number of moving groups outside of ~ 2 kpc in the "null" simulation, one may attribute the primary formation of moving groups at larger radii to dynamical interactions with dwarf

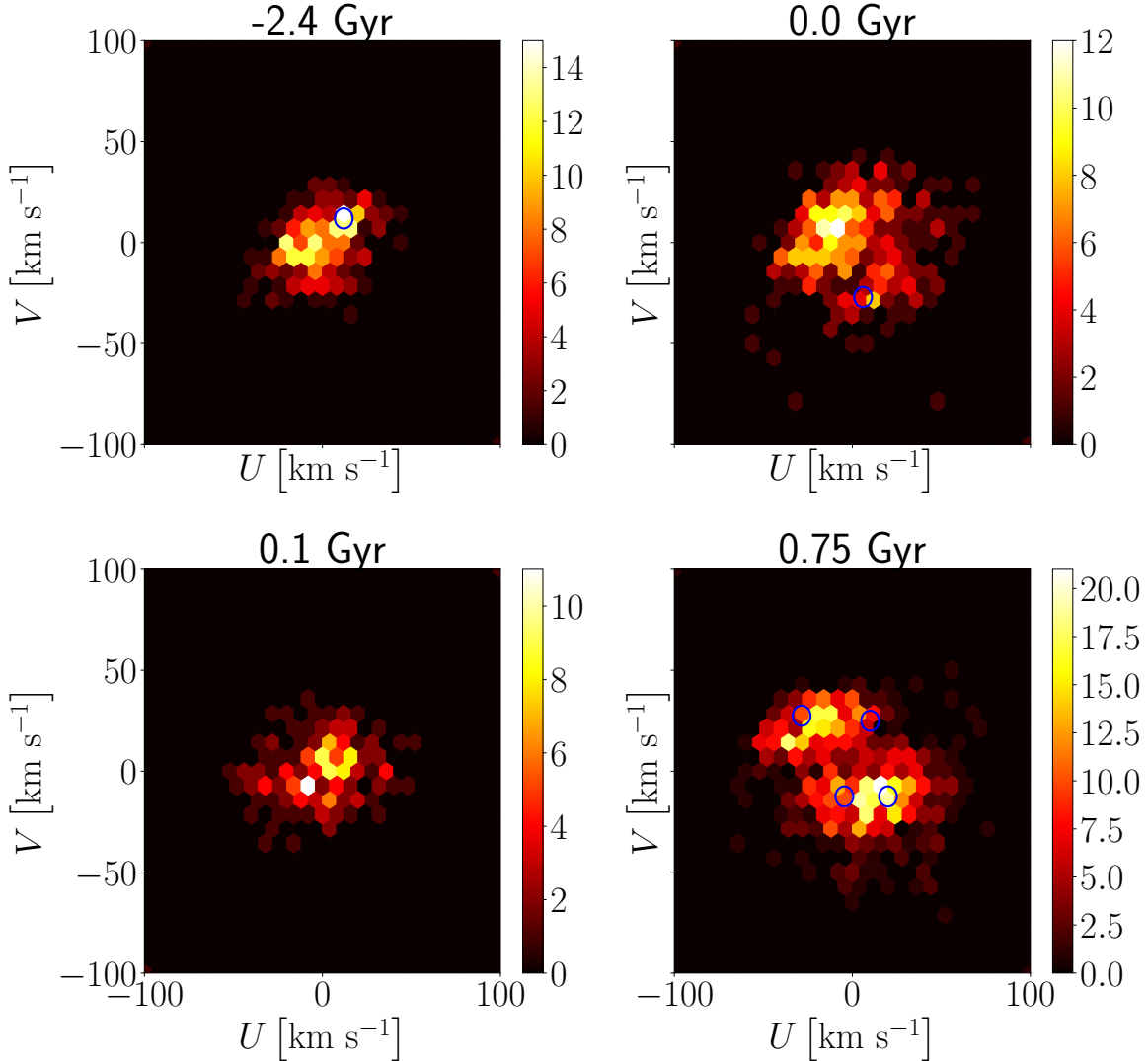


Figure 4. This figure is similar to Figure 3, however using the simulation with a dwarf galaxy on a Sagittarius-like orbit. The times shown are relative to present day, and we see similar results; there are clear velocity structures that form after present day in the simulations, which is again after the interaction has had time to perturb the disk. This is the same region of the disk as shown in Figure 3

galaxies in our simulations. The number of groups in the interacting simulations is also higher interior to ~ 2 kpc relative to the null case, which suggests that the dynamical interaction may be the primary cause at small radii as well.

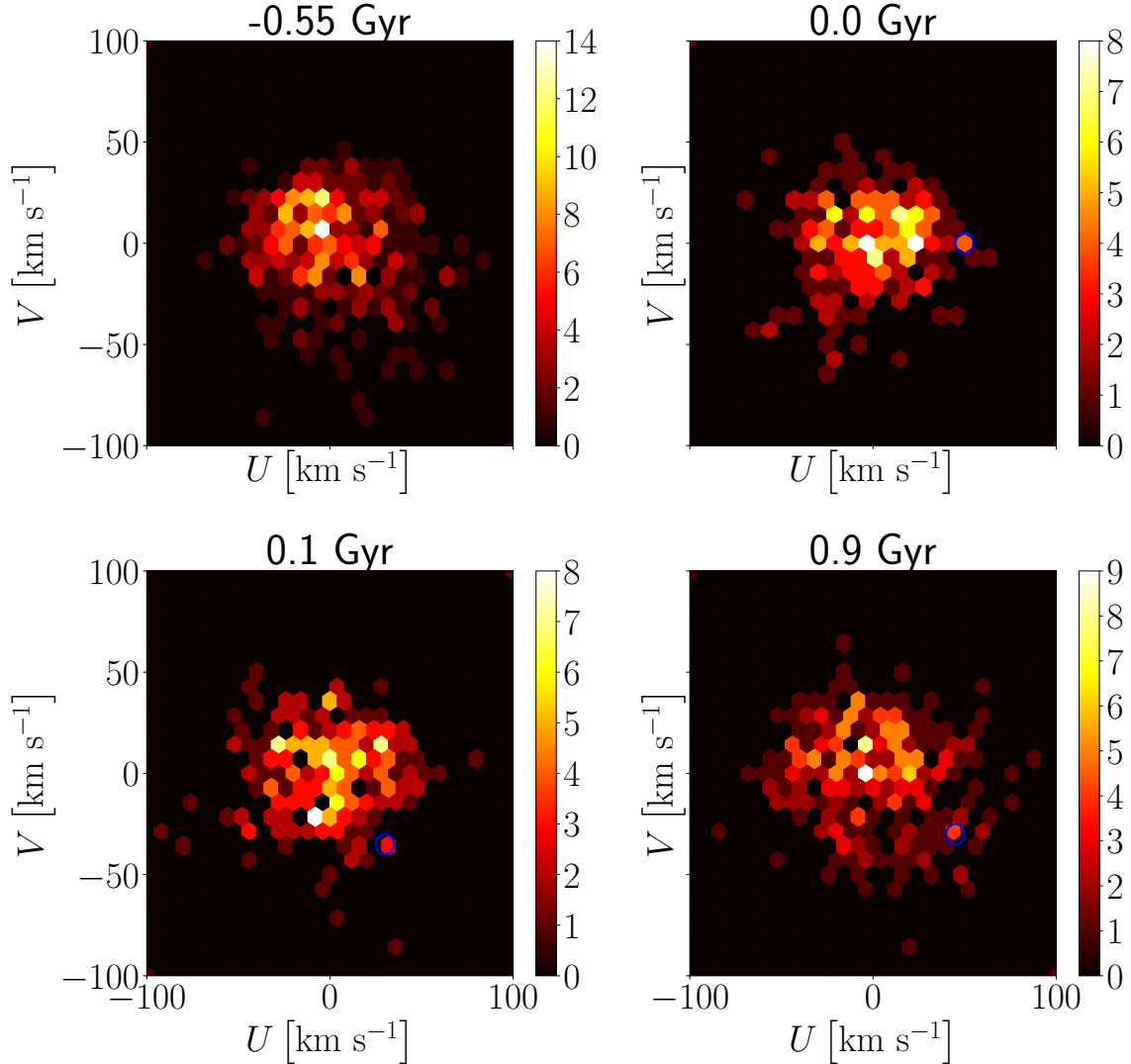


Figure 5. Velocity heat maps for the case with no dwarf galaxy. Here we see a lack of clear group formation, as we would expect. This shows that the velocity structures present in simulations without the presence of a perturber are relatively uninteresting. Similar plots made with times taken throughout the simulation yield similar results, which is a clear indication that the structures we see in our interacting simulations are a result of the perturbation from the dwarf galaxy. The region shown is the same as the region shown in the previous two figures.

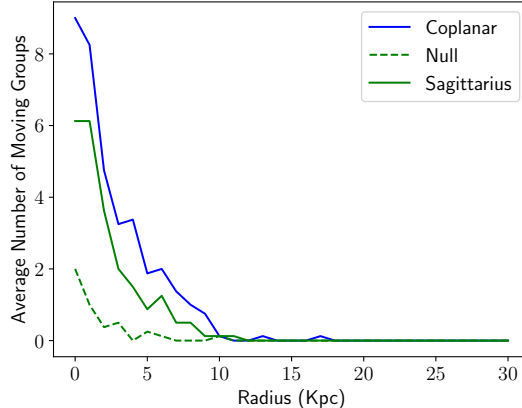


Figure 6. Average number of groups as a function of radius at present day. The results for the null simulation are plotted at the present day for both the co-planar and Sagittarius simulations. This shows that the two interacting simulations contain more groups detected by the algorithm than the null simulation does throughout the disk, indicating that many of the detected groups are a result of the perturbation.

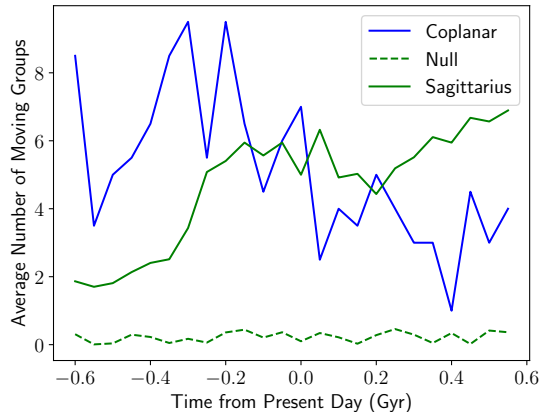


Figure 7. Average number of groups at 2 kpc as a function of time centered at present day. Here the two green curves are plotted at the present day of the Sagittarius simulation and the blue curve is at the present day of the co-planar simulation. There is some time dependence here in both interacting simulations, but no time dependence in the null case.

In a similar fashion, we can look at the time dependence of the average number of groups, which is shown in Figure 7. The same averaging procedure is used, with the number of groups calculated at eight different locations around the disk at a radius of 2 kpc. As before, the co-planar and Sagittarius simulations are examined at the present day, and we plot results from the null simulation centered at the present day of both of the other simulations. Following the stars present in one of the groups in these simulations over time is difficult; the groups fully deform over the course of one output time. The result is that the best time-dependent analysis available is one like this, where we track the number of structures over time instead of the evolution of individual structures. Note that in the co-planar case the closest approach has occurred before the earliest points in Figure 7, and the closest approach for the Sagittarius dwarf occurs after the data shown here.

The number of groups in the Sgr and co-planar simulations is comparable to a null simulation at early times ($t \sim -1$ Gyr or earlier), and increases appreciably after the interaction. On this scale, the point of closest approach in the Sagittarius simulation occurs at -0.3 Gyr from present day. In the CB09 simulation, the pericenter occurs 0.3 Gyr before present day. This is what one would expect if the groups are caused by the dwarf galaxy, as it takes about a

dynamical time for the gravitational perturbation to make a significant impact on the disk.

5. GROUP FINDING IN THE MILKY WAY

In order to confirm that this algorithm is effective, we use it to identify well-known groups observed within the Milky Way as a reference. We first looked for groups in the Hipparcos data. The hope is that the algorithm will be able to identify groups within a subset of the Hipparcos data, and provide parameters for the groups that agree with those that have been previously obtained.

One problem with group-finding using the data from Hipparcos is that there are no radial velocities in this data set, which prevents the calculation of three-dimensional space velocities, which are necessary for the algorithm to function. We can use other catalogues to obtain this information though; we used the Pulkovo compilation (Gontcharov 2006) of radial velocities for Hipparcos data, which includes 116,000 stars. This data set can be used to reproduce groups that have been known in the Milky Way, and makes a good sample set for testing the algorithm.

Figure 8 is a plot of the U, V velocities for stars in the Pulkovo compilation. In this plot there are four groups that are easily identified, and several rather small groups that are not readily apparent. Table 2 gives the parameters associated with these groups from Dehnen (1998), along with the output of the algorithm. In the table, we give the values of U and V for a variety of well known moving groups, as well as the resulting positions for the same groups that are output by the algorithm we use here. This shows that when we carry out our analysis on the RVs sample from Gaia DR-2, we do reproduce these locations to within reasonable tolerances. This table does not include the relative sizes of the groups, which was not included in the reference paper, and does not serve as a particularly good test of the algorithm.

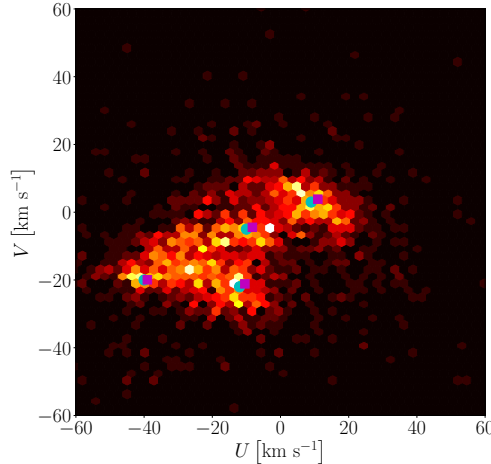


Figure 8. Velocities of stars in the Hipparcos Catalogue. Here we show the positions of known moving groups in the Milky Way and compare them to the groups detected by the algorithm. The cyan circles show the positions of known groups in the Milky Way, while the magenta squares show the locations of the same groups output by the algorithm.

6. COMPARISON OF SIMULATIONS WITH THE MILKY WAY

There are a large number of moving groups that are well known in the Milky Way that can readily be compared to the moving groups in our simulations. Many such groups were originally found in Hipparcos data, and more recently can be seen in Gaia data. Such groups include the Pleiades, Hyades, and Coma Bernices. In tests of our algorithm, these groups were easily detected in both the Hipparcos and Gaia data for stars near the Sun. There are some groups

Name	U	V	Algorithm U	Algorithm V
Pleiades	-12	-22	-11.7	-22.4
Hyades	-40	-20	-40.3	-21.2
Sirius & UMa	9	3	9.7	2.6
Coma Berenices	-10	-5	-9.5	-5.7
Group A			-25	-25
Group B			-81	-27
Group C			-59	52
Group D			-49	82
Group E			83	34
Group F			0	30
Group G			5	28
Group H			-30	32

Table 2. This table shows the positions of moving groups determined by the algorithm within Gaia DR-2. Those that are named in [Dehnen \(1998\)](#) have their names listed here, along with the coordinates given there. U and V are previously determined velocities, while Algorithm U and V are determined by our algorithm.

that prove to be problematic for the algorithm to identify, such as the NGC 1901 group, which is fairly small and close to the center of the background distribution. This group represents a weak point of the algorithm, which is that the algorithm has greater difficulty in identifying groups near the center of the background distribution. It is still generally successful in these regions, but occasionally struggles on small groups like NGC 1901.

Comparing the groups found in simulations with these groups in the Milky Way is not straightforward because the number of stars in the Solar neighborhood in the Milky Way is larger than in the comparable region in the simulations. However, we can directly compare the sizes of the observed groups and their standard deviations with the simulations. The moving groups in the simulations are roughly the same size as the moving groups in the Milky Way. The simulations occasionally produce moving groups with larger standard deviations than what we see in the Milky Way, with the largest standard deviations being larger by a factor of three. However, these groups make up a small minority of the total sample of groups within the simulations. The remaining groups have no clear features that distinguish them from groups that are observed in the Milky Way. One difference is that we do not see many very small groups in the simulations, but there are a few in the Milky Way such as NGC 1901 ([Dehnen 1998](#)). This may be due to the fact that there fewer star particles in the simulated Solar neighborhood region than in the observed Milky Way. Finally, the number of moving groups in the interacting simulations is less than in the Milky Way, by about 50 %; at $r = 2$ kpc, the fraction of moving groups in the co-planar simulation is 58 %, while for the Sgr interaction the relative fraction is 42%.

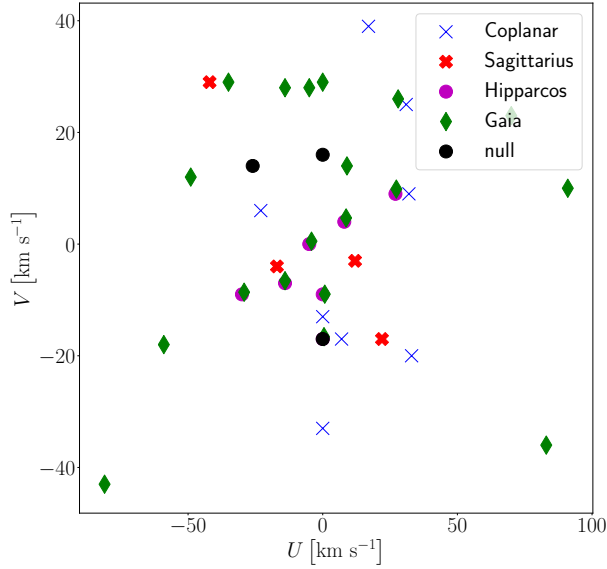


Figure 9. This scatter plot shows the locations of moving groups in Hipparcos data, the Sagittarius simulation and in the co-planar simulation. The spread of velocities of groups within these data sets shows that the spread within the Gaia data is appreciably greater than that of Hipparcos. Our simulations match the spread in the Gaia data quite well in the V direction, but is somewhat smaller in the U direction.

Figure 9 depicts the locations of moving groups in Hipparcos and Gaia data, as well as in the three simulations that we have analyzed here, shown at present day. Relative to the older Hipparcos data, the Gaia data has a larger spread in both the U and V directions, by a factor of almost 3. The Gaia data has a spread in U velocities that is about a factor of 2 larger than what is manifest in the co-planar simulation, while the spread in V for this simulation agrees with that in Gaia DR-2 to better than 10 %. The simulation with the three satellites has a spread in U that agrees with the Gaia data to better than a factor of 2, while the spread in V is within 25 % for this case, as opposed to the co-planar case which agrees nearly exactly with the spread in the Gaia data. The null simulation in both U and V is discrepant with the Gaia data, at the level of a factor of 4 and a factor of 1.4 respectively. While the simulations that we have analyzed here do not span a large enough parameter space for us to draw definitive conclusions, the comparison of the spread in $U - V$ velocities in the Gaia DR-2 data with the interacting simulations raises the question whether it may be possible to characterize dwarf galaxy interactions (to some extent) by analyzing the spread in the moving group structures formed by such interactions.

7. DISCUSSION & CONCLUSION

In this paper, we have compared moving groups identified in a series of simulations with data from the Milky Way, using an algorithm that we developed to identify groups in the U - V plane. Without a dwarf galaxy interaction, there is significantly less group formation in the simulation when compared to a simulation that includes a perturber, which suggests that the formation of these groups requires a gravitational interaction from a perturbing object. The groups begin to appear in the disk within a dynamical time after the collision. There is some preliminary indication that the parameters of the perturber have some impact on the properties of the groups, but additional analysis will be required to identify these dependencies. Without a dwarf galaxy, the algorithm still produces occasional results, but finds an average of 0.1 structures per data set, which is appreciably lower than what we find in the interacting simulations.

Our simulations do not generate as many moving groups as we observe around the Sun in the Milky Way. For example, at $r \sim 2$ kpc, there are about 50 % as many moving groups in our interacting simulations as there are in the Milky Way. There are likely several reasons for this. It is likely that this difference is due to the number of perturbing mechanisms, both external and internal to the Galaxy. A larger number of perturbation sources (i.e., in addition to

dwarf galaxies, such as globular clusters or molecular clouds or bars) may very well be able to produce a larger number of moving groups, and thus produce something closer to that observed in the Milky Way. None of the simulations form a bar, so none of the moving groups in the simulations are formed from a bar interaction. This can explain why we see fewer groups in the simulations than we do in the Gaia data. Moving groups can also be formed due to open cluster remnants. We can distinguish between groups that are open cluster remnants and dynamically formed groups by comparing the ages of the stars in the groups. If the stars have a wide range of ages, then it most likely formed through some kind of dynamic process, such as a dwarf galaxy perturbation. It is also likely that we would produce more moving groups in the simulations by increasing the resolution. The groups themselves in general are quite similar between observations and simulations, i.e., the sizes and standard deviations of the groups are typically within a factor of two relative to the observed values.

Another feature that is worth mentioning is the spread of the moving groups in the U-V plane. In the Hipparcos data, the moving groups are centered relatively close to the LSR. In our simulations, this is not the case, in fact there are groups that extend tens of kilometers per second beyond the farthest groups found within Hipparcos, particularly in the V direction. Using the Gaia data, this discrepancy reverses, with the observed data having a higher spread in the V direction, which is a better match to the results in our simulations, particularly those of the co-planar interaction modeled by [Chakrabarti & Blitz \(2009\)](#), which has parameters similar to the Antlia 2 interaction ([Chakrabarti et al. 2019](#)). If this spread in V velocities is distinct to the co-planar interaction, and is not characteristic of other interactions (as the Sgr dwarf interaction), it suggests that velocity tracers of the predicted dwarf galaxy from [Chakrabarti & Blitz \(2009\)](#) are now present in the Gaia DR-2 data set but not in the older Hipparcos data set.

Part of this work was conducted at the KITP Santa Barbara long-term program "Dynamical Models for Stars and Gas in Galaxies in the Gaia Era". SC and HN gratefully acknowledge the hospitality of the KITP during their visit, and NSF PHY-1748958. The simulations have been performed on Xsede, NERSC, and on Google Cloud. SC gratefully acknowledges support from NASA ATP NNX17AK90G, NSF AAG grant 1517488, and from Research Corporation for Scientific Advancement's Time Domain Astrophysics Scialog. HN acknowledges support from NSF grants AST 16-15688 and AST 19-08653. This work has made use of data from the European Space Agency (ESA) mission *Gaia* (<https://www.cosmos.esa.int/gaia>), processed by the *Gaia* Data Processing and Analysis Consortium (DPAC, <https://www.cosmos.esa.int/web/gaia/dpac/consortium>). Funding for the DPAC has been provided by national institutions, in particular the institutions participating in the *Gaia* Multilateral Agreement.

REFERENCES

Besla, G., Kallivayalil, N., Hernquist, L., et al. 2012, MNRAS, 421, 2109

Chakrabarti, S., Bigiel, F., Chang, P., & Blitz, L. 2011, ApJ, 743, 35

Chakrabarti, S., & Blitz, L. 2009, MNRAS, 399, L118

Chakrabarti, S., Chang, P., Price-Whelan, A., et al. 2019, arXiv e-prints, arXiv:1906.04203

Chang, P., & Chakrabarti, S. 2011, MNRAS, 416, 618

Dehnen, W. 1998, AJ, 115, 2384

—. 2000a, AJ, 119, 800

—. 2000b, AJ, 119, 800

Eggen, O. J. 1965, Moving Groups of Stars (the University of Chicago Press), 111

ESA, ed. 1997, ESA Special Publication, Vol. 1200, The HIPPARCOS and TYCHO catalogues. Astrometric and photometric star catalogues derived from the ESA HIPPARCOS Space Astrometry Mission

Gaia Collaboration, Prusti, T., de Bruijne, J. H. J., et al. 2016, A&A, 595, A1

Gaia Collaboration, Brown, A. G. A., Vallenari, A., et al. 2018, A&A, 616, A1

Gontcharov, G. A. 2006, Astronomy Letters, 32, 759

Hunt, J. A. S., Hong, J., Bovy, J., Kawata, D., & Grand, R. J. J. 2018, MNRAS, 481, 3794

Katz, D., Sartoretti, P., Cropper, M., et al. 2019, A&A, 622, A205

Khanna, S., Sharma, S., Tepper-Garcia, T., et al. 2019a, arXiv e-prints, arXiv:1902.10113

—. 2019b, MNRAS, 489, 4962

Laporte, C. F. P., Johnston, K. V., Gómez, F. A., Garavito-Camargo, N., & Besla, G. 2018, MNRAS, 481, 286

Laporte, C. F. P., Minchev, I., Johnston, K. V., & Gómez, F. A. 2019, MNRAS, 485, 3134

Levine, E. S., Blitz, L., Heiles, C., & Weinberg, M. 2006, arXiv e-prints, astro

Lipnicky, A., & Chakrabarti, S. 2017, in American Astronomical Society Meeting Abstracts, Vol. 229, American Astronomical Society Meeting Abstracts #229, 123.07

Quillen, A. C., Dougherty, J., Bagley, M. B., Minchev, I., & Comparetta, J. 2011, MNRAS, 417, 762

Quillen, A. C., Minchev, I., Bland-Hawthorn, J., & Haywood, M. 2009, MNRAS, 397, 1599

Quillen, A. C., Carrillo, I., Anders, F., et al. 2018a, MNRAS, 480, 3132

Quillen, A. C., De Silva, G., Sharma, S., et al. 2018b, MNRAS, 478, 228

Ramos, P., Antoja, T., & Figueras, F. 2018, A&A, 619, A72

Soubiran, C., Jasniewicz, G., Chemin, L., et al. 2018, A&A, 616, A7

Springel, V. 2005, MNRAS, 364, 1105

Springel, V., Di Matteo, T., & Hernquist, L. 2005, MNRAS, 361, 776

Springel, V., & Hernquist, L. 2003, MNRAS, 339, 289

Xu, Y., Newberg, H. J., Carlin, J. L., et al. 2015, ApJ, 801, 105